

## STAR FORMATION EFFICIENCY IN LOW SURFACE BRIGHTNESS REGIONS

F. Combes<sup>1</sup>

**Abstract.** Low surface brightness regions are found not only in dwarf and ultra-diffuse galaxies, but also on the outer parts of giant spirals, or in galaxy extensions (tidal or ram-pressure tails, outflows or jets). Sometimes molecular gas is detected in sufficient quantities to allow star formation, but the efficiency is much lower than in disk galaxies. This presentation reviews different environments showing low-surface brightness, their gas content and surface densities, and their star formation efficiency. Some interpretations are proposed to account for this low efficiency.

Keywords: Galaxies, Star formation, Molecular clouds, Ram-pressure, Cooling flow cluster

### 1 XUV disks

The extended ultraviolet disks (XUV disks) have been discovered by the GALEX satellite, and are characterized by UV emission well beyond the optical disk, traced by an H $\alpha$  emission drop. A prototypical example of XUV disks is the galaxy M83 (Thilker et al. 2005). To explore the star formation efficiency in the outer parts of the galaxy, we conducted ALMA observation in CO(2-1) of the M83 XUV disk, with a spatial resolution of 17pc x 13pc, well adapted to detect Giant Molecular Clouds (GMC). Although a significant region was observed (about 2 x 4 kpc) with a 121 point mosaic (see Figure 1), and although the region includes several HII regions and is rich in HI-gas, no CO emission was detected (Bicalho et al. 2019). This result is surprising, especially since we detected CO emission in another XUV disk with the IRAM-30m, e.g. in M63 (Dessauges-Zavadsky et al. 2014).

A compilation of all results from the literature is plotted in the Kennicutt-Schmidt diagram of Figure 2, in comparison with normal galaxies. This diagram is focussed on the H<sub>2</sub> gas, and shows the depletion time of the local main sequence galaxies of  $2 \times 10^9$  yrs (Bigiel et al. 2008). The outer disks of M63, NGC 6946 and NGC 4625 have a much larger depletion time, or equivalently a much lower star formation efficiency (SFE), by several orders of magnitude. As for M83, globally the large region observed will also have a low SFE; however, if we consider the two main HII regions, of size  $\sim 200$ pc, and compute the upper limits of CO emission, the non detection is an exception (cf Figure 2). This absence of CO cannot be attributed solely to a low metallicity, since the gas abundance in this region is half solar (Bresolin et al. 2009). It is possible that in these outer regions, molecular clouds are not enough shielded from the UV field, and the CO molecules are photo-dissociated, while the H<sub>2</sub> is still there. Clouds could be smaller, and the carbon mostly in C and C<sup>+</sup>.

### 2 Cooling filaments

Another situation where the SFE is low involves gas flows in cool core clusters. The prototype is the Perseus cluster, where H $\alpha$  filaments are known since a long time, most of them excited by shocks, but in some places by star formation (Canning et al. 2014). The hot X-ray gas reveals large cavities, sculpted by the central AGN with its radio jets (Fabian et al. 2011). It is now well established that the AGN feedback moderates the gas cooling, and cold molecular gas is detected around the cavities (Salomé et al. 2006). The gas is still raining down around the cavities towards the AGN to fuel it. CO and H $\alpha$  emissions are well correlated in cool core clusters (Salomé & Combes 2003). There is a relation between the star formation rate (SFR) and the gas cooling rate with a slope larger than unity for strong cooling rates (McDonald et al. 2018). For low cooling rate, however (lower than 30 M<sub>⊙</sub>/yr) SFR and cooling rate are not correlated, pointing to SFR fueled by recycled gas then. The star formation efficiency may then be low; globally, for the Perseus cluster, it is not far from the mean, as seen in Figure 3.

<sup>1</sup> Observatoire de Paris, LERMA, Collège de France, CNRS, PSL Univ., Sorbonne Univ., Paris

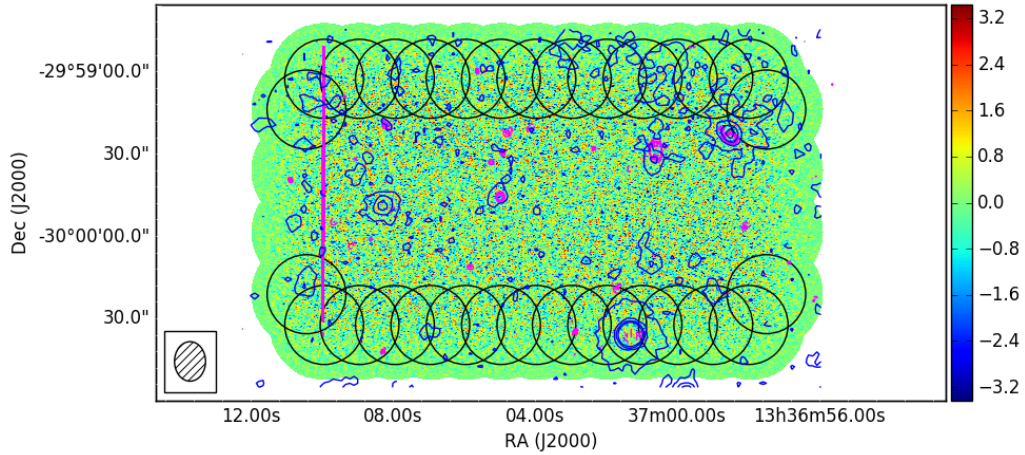


**Fig. 1.** Schematic representation of the 121-point mosaic of the ALMA observations, in the XUV disk of M83. The black circles indicate some of the 27''-diameter primary beams of the CO(2-1) emission. In the background, the color map is the moment zero of the CO(2-1) data cube. The magenta contours are H $\alpha$  and the black contours are FIR 24 $\mu$ m emission. From Bicalho et al. (2019).

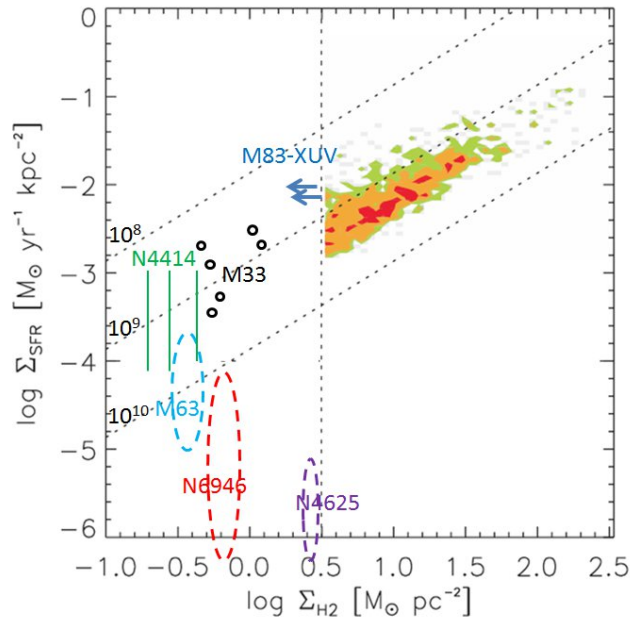


**Fig. 2.** Resolved Kennicutt-Schmidt diagram, in several galaxies and low surface brightness regions, adapted from Bigiel et al. (2008) and Verdugo et al. (2015). Dashed ovals indicate the location of XUV disk galaxies. The vertical dash line, at 3  $M_{\odot}/\text{pc}^2$  corresponds to the sensitivity limit of the CO data in Bigiel et al. (2008). Depletion times of  $10^8$ ,  $10^9$  and  $10^{10}$  years are represented by 3 inclined dashed lines. When considering two of the main H $\alpha$  regions, of  $\sim 200\text{pc}$  size, and the upper limits on their molecular gas surface density, we obtain the blue horizontal arrows in M83. From Bicalho et al. (2019).

### 3 Ram-pressure stripped tails

In galaxy clusters, galaxies suffer tidal and ram-pressure stripping from the Intra-Cluster-Medium (ICM), and lose their gas which constitutes a diffuse circum-galactic medium. This loss of gas leads to what is called environmental quenching of star formation. The importance of this quenching depends on the richness of the cluster. Ram pressure is relative mild in the Virgo cluster, where many spirals are HI deficient, but not perturbed

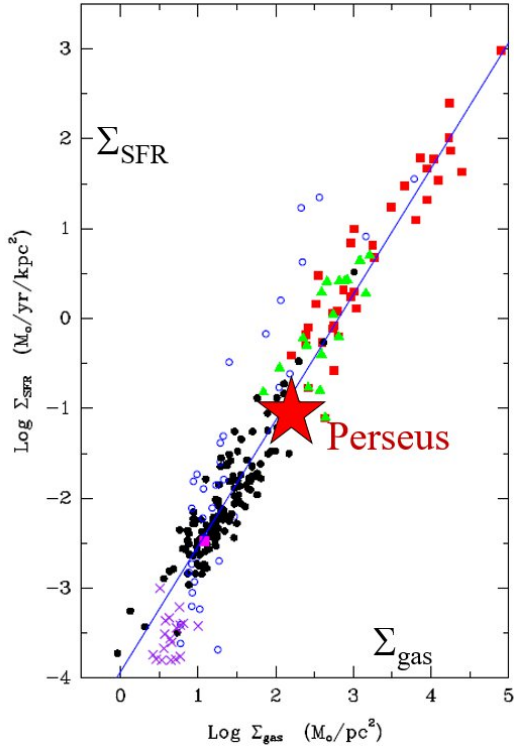


**Fig. 3.** The position of Perseus cluster in the global Kennicutt-Schmidt diagram is indicated as a large red star, and compared to local main sequence galaxies and starbursts (Kennicutt & Evans 2012).

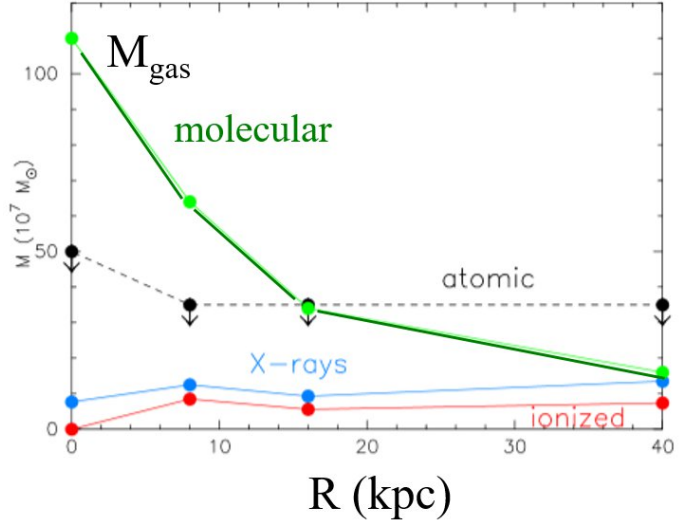


**Fig. 4.** Radial distribution of the various gas phases in ESO137-001: the molecular gas in green, the atomic HI gas in black (upper limits), the X-ray gas in blue, and the H $\alpha$  gas in red. From Jáchym et al. (2014).

in their molecular gas (Kenney & Young 1989).

There is however a giant H $\alpha$  tail in the center of Virgo linking the NGC 4438 galaxy to M86, over scales  $\sim 100$  kpc (Kenney et al. 2008). Although M86 is a lenticular galaxy devoid of gas, there is CO emission detected at 10kpc south of this galaxy, in prolongation of the long tail from NGC 4438. Apparently, this gas comes from the latter spiral. It is surprising to find  $2 \cdot 10^7 M_{\odot}$  of H $_2$  gas in such an hostile environment, embedded in hot  $10^7$ K ICM gas. Either the H $_2$  molecules have survived during the 100 Myr path, or they were re-formed in situ (Dasyra et al. 2012).

One of the H $\alpha$  tail, linking NGC 4388 and M86 is rich in HI gas. Verdugo et al. (2015) have detected CO emission in some of the clumps along the tail. When plotted on the Kennicutt-Schmidt diagram, as in Fig. 2, the star formation efficiency is much lower there than in galaxy disks, similar to XUV disks (Verdugo et al. 2015). It is possible that the gas in the tail is more 3D distributed than in 2D-like disks, and also they are lacking the pressure from the gravity of disk stars.

In richer galaxy clusters, such as the Norma or Coma clusters, ram-pressure can strip the gas from galaxies much faster: this is the case of ESO137-001 (Jáchym et al. 2014). The tail of 80kpc is spectacular and double in X-ray emission, and in H $\alpha$ . CO emission has been detected easily all along the double-tail, and the molecular gas dominates the gas content, as shown in Figure 4. The total molecular content of the tail, a few  $10^9 M_{\odot}$  is larger than the molecular content of the galaxy disk itself. ALMA has shown that the tail emission is very clumpy, and that the molecular gas is reforming in situ (Jachym et al. 2019). The galaxy D100 in Coma has a similar ram-pressure tail, remarkably straight, and consisting of only one thin component starting from the galaxy center, as shown by MUSE (Fumagalli et al. 2014). This is expected from a later stage of stripping. Again the molecular gas dominates in mass the gaseous tail (Jáchym et al. 2017), but the SFE is much lower than in normal galaxy disks.

#### 4 Importance of pressure

In all these low surface density environments, the SFE is found much lower than in normal disks. This suggests that the surface density of stars is very important for the star formation efficiency. Already Shi et al. (2011) have shown that the SFE in all kinds of environments is strongly correlated to the stellar surface density, and much less on the gas surface density. The HI to H<sub>2</sub> transition is favored by external pressure (Blitz & Rosolowsky 2006).

An example of radio jet-induced star formation in Centaurus A have indeed demonstrated that the HI gas is preferentially transformed in molecular gas on the jet passage (Salomé et al. 2016). Here again the SFE is much lower than normal, the depletion time in the induced star forming region is between 7 and 16 Gyr.

#### 5 Conclusions

There are several environments showing low surface brightness in stars: not only dwarf and ultra-diffuse galaxies, but also the outer parts of galaxies, or stars belonging to circum-galactic regions, either from a cooling flow, or in tidal and ram-pressure stripped tails. In all these environments, XUV disks, cooling filaments in cool-core clusters, or ram-pressure tails, the disk pressure due to the gravity of stars is deficient or non-existing. First, the gas is not confined in a thin disk, and the star formation might be not only proportional to the gas surface density, but to the volumic gas density, which is then lower. But also the stellar pressure is missing to trigger the transformation of diffuse atomic gas to dense molecular gas, which reduces the efficiency of star formation. Even in hostile environments like the hot ICM medium, the molecular gas is resilient and can form in situ, in cooling filaments, in ram-pressure stripped tails. Star formation is observed, but with a low efficiency.

I thank Samuel Boissier for having organised such an interesting workshop.

#### References

- Bicalho, I. C., Combes, F., Rubio, M., Verdugo, C., & Salomé, P. 2019, *A&A*, 623, A66  
 Bigiel, F., Leroy, A., Walter, F., et al. 2008, *AJ*, 136, 2846  
 Blitz, L. & Rosolowsky, E. 2006, *ApJ*, 650, 933  
 Bresolin, F., Ryan-Weber, E., Kennicutt, R. C., & Goddard, Q. 2009, *ApJ*, 695, 580  
 Canning, R. E. A., Ryon, J. E., Gallagher, J. S., et al. 2014, *MNRAS*, 444, 336  
 Dasyra, K. M., Combes, F., Salomé, P., & Braine, J. 2012, *A&A*, 540, A112  
 Dessauges-Zavadsky, M., Verdugo, C., Combes, F., & Pfenniger, D. 2014, *A&A*, 566, A147  
 Fabian, A. C., Sanders, J. S., Allen, S. W., et al. 2011, *MNRAS*, 418, 2154  
 Fumagalli, M., Fossati, M., Hau, G. K. T., et al. 2014, *MNRAS*, 445, 4335  
 Jáchym, P., Combes, F., Cortese, L., Sun, M., & Kenney, J. D. P. 2014, *ApJ*, 792, 11  
 Jáchym, P., Kenney, J. D. P., Sun, M., et al. 2019, arXiv e-prints, arXiv:1905.13249  
 Jáchym, P., Sun, M., Kenney, J. D. P., et al. 2017, *ApJ*, 839, 114  
 Kenney, J. D. P., Tal, T., Crawl, H. H., Feldmeier, J., & Jacoby, G. H. 2008, *ApJ*, 687, L69  
 Kenney, J. D. P. & Young, J. S. 1989, *ApJ*, 344, 171  
 Kennicutt, R. C. & Evans, N. J. 2012, *ARA&A*, 50, 531  
 McDonald, M., Gaspari, M., McNamara, B. R., & Tremblay, G. R. 2018, *ApJ*, 858, 45  
 Salomé, P. & Combes, F. 2003, *A&A*, 412, 657  
 Salomé, P., Combes, F., Edge, A. C., et al. 2006, *A&A*, 454, 437  
 Salomé, Q., Salomé, P., Combes, F., & Hamer, S. 2016, *A&A*, 595, A65  
 Shi, Y., Helou, G., Yan, L., et al. 2011, *ApJ*, 733, 87  
 Thilker, D. A., Bianchi, L., Boissier, S., et al. 2005, *ApJ*, 619, L79  
 Verdugo, C., Combes, F., Dasyra, K., Salomé, P., & Braine, J. 2015, *A&A*, 582, A6